First-principles investigation on the elastic stability and thermodynamic properties of Ti_2SC*

Yang Ze-Jin(杨则金)[a)†], Guo Yun-Dong(郭云东)[b)], Linghu Rong-Feng(令狐荣锋)[c)], Cheng Xin-Lu(程新路)[d)], and Yang Xiang-Dong(杨向东)[d)]

[a)] *School of Science, Zhejiang University of Technology, Hangzhou* 310023, *China*

[b)] *School of Physics, Neijiang Normal University, Neijiang* 641112, *China*

[c)] *School of Physics, Guizhou Normal College, Guiyang* 550018, *China*

[d)] *Institute of Atomic and Molecular Physics, Sichuan University, Chengdu* 610065, *China*

(Received 15 November 2011; revised manuscript received 12 December 2011)

Using Vanderbilt-type plane-wave ultrasoft pseudopotentials within the generalized gradient approximation (GGA) in the frame of density functional theory (DFT), we have investigated the crystal structures, elastic, and thermodynamic properties for Ti_2SC under high temperature and high pressure. The calculated pressure dependence of the lattice volume is in excellent agreement with the experimental results. The calculated structural parameter of the Ti atom experienced a subtle increase with applied pressures and the increase suspended under higher pressures. The elastic constants calculations demonstrated that the crystal lattice is still stable up to 200 GPa. Investigations on the elastic properties show that the c axis is stiffer than the a axis, which is consistent with the larger longitudinal elastic constants (C_{33}, C_{11}) relative to transverse ones (C_{44}, C_{12}, C_{13}). Study on Poisson's ratio confirmed that the higher ionic or weaker covalent contribution in intra-atomic bonding for Ti_2SC should be assumed and the nature of ionic increased with pressure. The ratio (B/G) of bulk (B) and shear (G) moduli as well as B/C_{44} demonstrated the brittleness of Ti_2SC at ambient conditions and the brittleness decreased with pressure. Moreover, the isothermal and adiabatic bulk moduli displayed opposite temperature dependence under different pressures. Again, we observed that the Debye temperature and Grüneisen parameter show weak temperature dependence relative to the thermal expansion coefficient, entropy, and heat capacity, from which the pressure effects are clearly seen.

Keywords: first-principles, elasticity, thermodynamic properties, Ti_2SC

PACS: 63.20.dk, 62.20.D–, 65.40.–b **DOI:** 10.1088/1674-1056/21/5/056301

1. Introduction

The $M_{n+1}AX_n$ phases, where M is an early transition metal, A is an A-group element (mostly IIIA and IVA elements), X is either C or N and n varies from 1 to 3, have attracted more and more attention during recent years due to the fundamental properties usually associated with metals and ceramics.[1] Their excellent electronic properties[2,3] are comparable to or higher than those of the constituent transition metals, which had not been anticipated till now.[4] In addition, their unusual mechanical properties have also been extensively utilized in industry production.[5,6] The unique combination of metallic and ceramic properties including high strength and stiffness under high temperatures, resistance to oxidation and thermal shock, as well as high Young's modulus, low hardness, and ultra-low solid friction coefficients etc.[1,7−13] are promising for high-temperature applications.

Furthermore, for some nanolaminates, low-temperature superconductivity was discovered.[4,14−17] As we all know, the structural parameter of the M atom ($M_{n+1}AX_n$) shifts with pressure and thus behaves with a different variation mechanism relative to the other hexagonal lattice with similar structures. Under pressure, elements usually become denser as the atoms and molecules get closer together and the occupied volume decreases, non-metals becoming metals and even superconductors.[18] Under high

*Project supported by the National Natural Science Foundation of China (Grant Nos. 10974139, 10964002, 11104247, and 11176020), the Natural Science Foundation of Guizhou Province, China (Grant Nos. [2009]2066 and [2009]07), the Project of Aiding Elites' Research Condition of Guizhou Province, China (Grant No. TZJF-2008-42), and the Science Foundation from Education Ministry of Zhejiang Province, China (Grant No. Y201121807).

†Corresponding author. E-mail: yzjscu@163.com

© 2012 Chinese Physical Society and IOP Publishing Ltd

pressure, the light alkali elements Li[19] and Na[20] undergo unusual metal-to-semiconductor transition. Moreover, the transparent dense sodium[20] is particularly striking as it has challenged the traditional theory. Also, a new ultra-hard form of carbon may exist between graphite and diamond.[21] To date, more than 50 M_2AX compounds have been determined.[1] Ti_2SC, a member of the M_2AX compounds, has recently attracted increasing attention due to its unique structural characteristics.[12,22] Very recently, the fully dense Ti_2SC was synthesized[12,22] and it exhibits the highest thermal conductivity and Young's modulus at room temperature. Sulfur containing ternaries, as well as P and As, have a considerably shorter c-axis lattice parameter than those of the other MA_2X compounds. This results in the lowest c/a ratio of the M_2AX compounds and is thus expected to exhibit different properties. For instance, Nb_2SC is a known superconductor, with a transition temperature of 3–5 K depending on C concentration.[15]

Recently, first-principles calculations have been successfully used to reveal and predict the structural, mechanical, and physical properties of many M_2AX phases.[23–25] The electronic structure,[25–27] as well as the elastic[26–28] and thermodynamic[28] properties (under ambient conditions) of Ti_2SC has been calculated. The equation of the state of Ti_2SC has been measured[29] by synchrotron radiation X-ray diffraction under pressure to 47 GPa, and the hardness[12] has been determined to be 8 GPa. However, the detailed theoretical studies on elastic properties and thermodynamic properties under high temperature and high pressure have never been fully investigated. Therefore, it is necessary to carry out an extensive investigation on the elastic and thermodynamic properties for Ti_2SC to reveal the origin of the excellent properties. First-principles calculations[30–43] offer one of the most powerful tools for carrying out theoretical studies of these properties.[18–20,44–50]

2. Computational methods

In the electronic structure calculations, we have used the non-local ultrasoft pseudopotential introduced by Vanderbilt,[51] together with the Perdew and Wang's PW91 generalized gradient approximation (GGA) exchange-correlation function.[52,53] The current selected computational model has been validated by the most recent experimental results.[29] Considering the computational cost, a plane-wave basis set with an energy cut-off 500.0 eV has been applied, and the 9×9×2 Monkhorst–Pack mesh has been used for the Brillouin-zone k-point sampling.[29] Pseudo atomic calculations have been performed for Ti $3s^2 3p^6 3d^2 4s^2$, S $3s^2 3p^4$, and C $2s^2 2p^2$, where the self-consistent convergence of the total energy is at 5.0×10^{-7} eV/atom. All the electronic calculations are performed by the Cambridge Serial Total Energy Package (CASTEP).[54,55] It is found that these model parameters are sufficient in leading to well converged total energy and geometrical configurations.[56,57]

3. Results and discussion

3.1. Geometry optimization

Ti_2SC crystallizes in the $P6_3/mmc$ (194) space group and there are 8 atoms[12,22,26,29] in one unit cell; the detailed crystal structure investigations have been reported elsewhere.[26,29] According to the space group constraints, the Ti atoms are located at (1/3, 2/3, z), S atoms at (1/3, 2/3, 3/4) and C atoms at (0, 0, 0). Thus, the stable geometry can be uniquely determined by the lattice constants a ($b = a$) and c, as well as the structural parameter z. The detailed optimization process for $P6_3/mmc$ space symmetric group has been extensively described elsewhere.[4,25] The optimized stable geometry with lattice parameters $a = b = 3.204$ Å, $c = 11.25$ Å, is consistent with the experimental data and other theoretical values and the optimized structural parameter of the Ti atom also agrees well with other theoretical reports (see Table 1 in details). The obtained pressure dependence of the lattice volume shows excellent agreement with experimental measurement,[29] as is shown in Fig. 1.

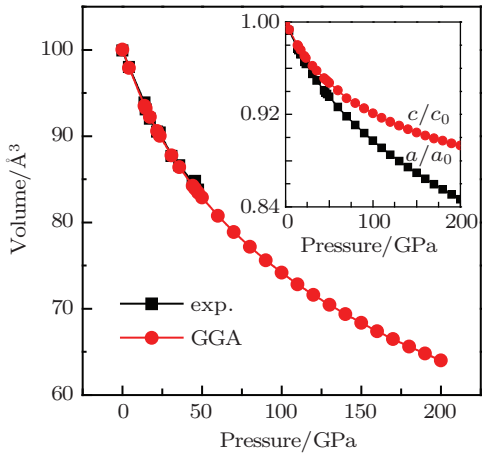


Fig. 1. (colour online) The obtained pressure-volume relations of Ti_2SC, the experimental data are taken from Ref. [29]. Insert is the normalized axial compressibility.

Table 1. The stable lattice parameter (Å) and the bulk modulus B_0 (GPa), shear modulus G (GPa) and Young's modulus E (GPa). Third-order Birch–Murnaghan ($P = (3/2)B_0[(V/V_0)^{-7/3} - (V/V_0)^{-5/3}]\{1-(3/4)(4-B')[(V/V_0)^{-2/3}-1]\}$) equation is used to fit B_0 and B' within 0–200 GPa.

Ti_2SC	a_0	c_0	u	c_0/a_0	B_0	B'	G	E	B/C_{44}
GGA/PW91	3.204	11.25	0.0988	3.5112	182.86	4.0	134.09	297.21	1.17
exp.[28]	3.204	11.211			145		125	290	
exp.[29]	3.208(1)	11.21(1)		3.4944	191(4)	4.0(0.3)			
exp.[68]	3.216	11.22		3.4888					
exp.[69]	3.2046(1)	11.2093(3)		3.498	191(3)		125		
exp.[12]	3.205	11.208		3.497	145		125	316(2)	
DFT[26]	3.211	11.239	0.0993		181		134	322	
DFT[63]	3.1432	11.0509	0.0998		204.08	4.22	150.0	363.0	
DFT[29]	3.21	11.29		3.5171	183	4.1			
DFT[12]	3.186	11.231	0.0993		176				
DFT[22]					145				
DFT[69]					179		139		
DFT[24,65]									1.2–1.7
DFT[24,70]									1.15–1.33
DFT[28]	3.205	11.264		3.515	179		138	329	
DFT[71]					181				
DFT[27]	3.206	11.236	0.0992	3.5047	179.85	4.13	124.81		
DFT[72]	3.208	11.27			177		134	321	

The experimental measurement[29] are performed up to 47.5 GPa; in order to investigate in depth the thermo-elastic dynamic stability under higher pressures, we have extended the pressure range to 200 GPa. From Fig. 1 we confirmed that the current selected computational methods are reliable, thus all of the following calculations are carried out by the same methods as GGA/PW91. Figure 2 reveals the structural parameter variations of the Ti atom with pressure by GGA/PW91 and localized density approximation for the Ceperly–Alder and Perdew–Zunger exchange-correlation function (LDA/CAPZ) (using the same accuracy with that of GGA method for confirmation purpose), respectively.

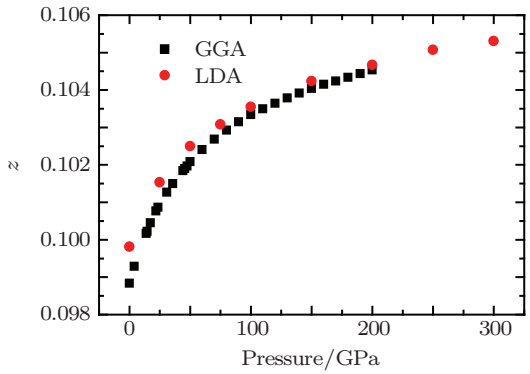


Fig. 2. (colour online) The structural parameter of the Ti atom varies with pressure.

3.2. Elastic properties

Elastic properties of solids are closely related to many fundamental solid-state properties, such as equation of state, specific heat thermal expansion, Debye temperature, Grüneisen parameter and so on. From the elastic constants, one can obtain important information about the binding characteristics, the anisotropic feature, and the structural stability. The calculated elastic constants are shown in Fig. 3, from which we can see that the five independent elastic constants behave with almost linear relationships with the applied pressures. The larger longitudinal elastic constants (C_{33}, C_{11}) relative to transverse ones (C_{44}, C_{12}, C_{13}) and the stiffer c-axis compressibility (shown in Fig. 1) than that of a-axis revealed that c-axis is much stiffer in Ti_2SC. Moreover, it is found that C_{11} and C_{33} vary more largely under pressure than those of C_{12}, C_{13}, and C_{44}. The C_{11} and C_{33} are related to the deformation behavior and atomic bonding characteristics. As is shown in Fig. 4, the current $C_{33} > C_{11}$ means that the atomic bonds along the [001] planes between nearest neighbors are stronger than those along the [100] plane. Besides, the larger C_{33}/C_{11} (1.0656) and smaller C_{13}/C_{12} (1.0586) mean that the atomic bonds along the c-axis are identical with those of a-axis at 0 GPa. The calculated elastic constants under different pressures are shown in Table 2. According to the well-known elastic stability

criteria,[58] i.e.,

$$C_{12} > 0, \quad C_{33} > 0, \quad (C_{11} - C_{12})/2 > 0,$$
$$C_{44} > 0, \quad (C_{11} + C_{12})C_{33} - 2C_{13}^2 > 0, \qquad (1)$$

we found that Ti_2SC is mechanically stable up to 200 GPa.

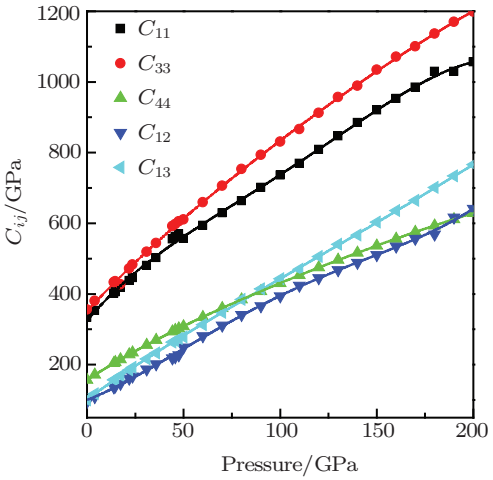


Fig. 3. (colour online) The elastic constants of Ti_2SC versus the external pressures at 0 K.

Table 2. The calculated elastic constants (GPa) of Ti_2SC, together with the other theoretical results at 0 GPa.

	C_{11}	C_{33}	C_{44}	C_{12}	C_{13}
Present	333	355	156	94	100
DFT[69]	339	354	162	90	100
DFT[63]	368(2)	395(1)	189(1)	108(2)	123(1)
DFT[26]	336	348	163	106	99
DFT[27]	318.51	351.11	148.56	101.42	105.79
DFT[72]	331	348	157	98	97

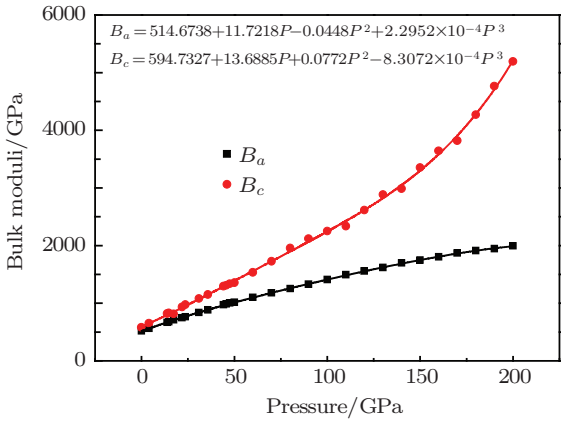


Fig. 4. (colour online) Axial bulk moduli of Ti_2SC at 0 K.

The mechanical anisotropy of Ti_2SC can be evaluated from the bulk moduli along the a and c axes, B_a and B_c, respectively,[59]

$$B_a = a\frac{\mathrm{d}P}{\mathrm{d}a} = \frac{\Lambda}{2+\alpha}, \qquad (2)$$

$$B_c = c\frac{\mathrm{d}P}{\mathrm{d}c} = \frac{B_a}{\alpha}, \qquad (3)$$

$$\Lambda = 2(C_{11} + C_{12}) + 4C_{13}^{\alpha} + C_{33}\alpha^2, \qquad (4)$$

$$\alpha = \frac{C_{11} + C_{12} - 2C_{13}}{C_{33} - C_{13}}. \qquad (5)$$

The calculated B_a and B_c with pressure are presented in Fig. 4. It seems that B_a and B_c increase linearly with pressure, and the former is always smaller than the latter. Further analysis shows that B_c/B_a tends to gradually increase with pressure, which may reveal that the mechanical behavior of Ti_2SC under pressure is of anisotropy.

It is known that the acoustic velocities are obtained from elastic constants by the Christoffel equation[60]

$$(C_{ijkl}n_jn_k - M\delta_{il})\mu_i = 0, \qquad (6)$$

where $M = \rho\nu^2$, C_{ijkl} is the fourth rank tensor description of the elastic constants, n is the propagation direction, and $\boldsymbol{\mu}$ is the polarization vector. The acoustic anisotropy is defined as[61]

$$\Delta_i = \frac{M_{i[n_x]}}{M_i[100]}, \qquad (7)$$

where n_x is the extremal propagation direction and i is the index of three types of elastic waves (one longitudinal and two traversal polarizations of shear waves). By solving the Christoffel equation for Ti_2SC, the anisotropy of the compression wave is calculated from

$$\Delta_P = \frac{V_l^2(0°)}{V_l^2(90°)} = \frac{C_{33}}{C_{11}}. \qquad (8)$$

The anisotropies of the wave polarized perpendicular to the basal plane (S_1) and to the basal plane (S_2) are calculated from

$$\Delta_{S_1} = \frac{C_{11} + C_{33} - 2C_{13}}{4C_{44}}, \qquad (9)$$

$$\Delta_{S_2} = \frac{V_t^2(0°)}{V_t^2(90°)} = \frac{2C_{44}}{C_{11} - C_{12}}. \qquad (10)$$

Where Δ_P shows the anisotropy of the compression wave, Δ_{S_1} and Δ_{S_2} denote the shear waves, $V(90°)$ and $V(0°)$ are the in-plane and c-axis ultrasound velocities, respectively. For an elastically isotropic solid, $\Delta_P = \Delta_{S_1} = \Delta_{S_2} = 1$. The obtained elastic anisotropy factors for Ti_2SC are shown in Fig. 5, from which we see that Δ_{S_2} increases rapidly and Δ_P increases slightly with pressure, whereas Δ_{S_1} decreases

with pressure. The different variation trends confirmed the anharmonicity of the acoustic vibrations.

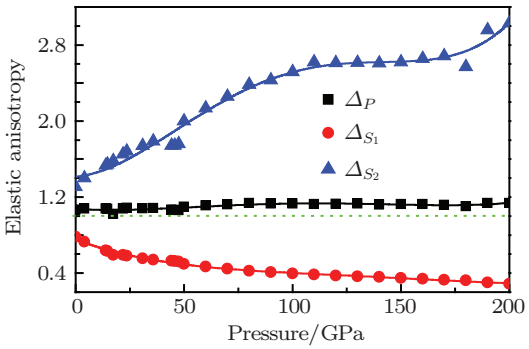


Fig. 5. (colour online) Elastic anisotropy of Ti_2SC at 0 K.

As we all know, the isothermal and adiabatic bulk moduli exist with small differences owing to the very small thermal expansion coefficient α and Grüneisen parameter γ, $B_S = B_T(1 + \alpha\gamma T)$. However, it is important to investigate the relations to reveal the effect under pressure and temperature. Our calculated isothermal and adiabatic bulk moduli variations with pressure and temperature are shown in Fig. 6. Through the present calculations we found that the adiabatic bulk modulus (B_S) increases with temperature at 0 GPa and then decreases under higher pressures. In contrast with B_S, the isothermal bulk moduli (B_T) displayed similar tendencies with only a minimum at 0 GPa. The current investigations confirmed that B_S is always larger than B_T over wide pressure and temperature ranges and both of them increase with pressure at 0 K.

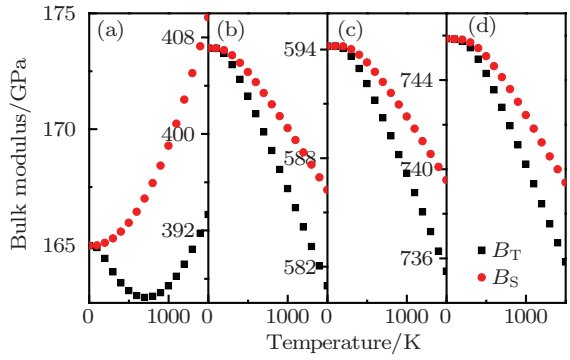


Fig. 6. (colour online) Isothermal (B_T) and adiabatic (B_S) bulk moduli of Ti_2SC under different temperatures and pressures: (a) 0 GPa, (b) 60 GPa, (c) 120 GPa, (d) 180 GPa.

3.3. Thermodynamic properties

Poisson's ratio is generally used to quantify the stability of the crystal against shear and provides more information about the characteristics of the bonding forces than the elastic constant. Usually it ranges from −1 to 0.5, the value of the Poisson's ratio for covalent materials is small ($\sigma = 0.1$), whereas for ionic materials a typical value[62] of σ is 0.25. In our cases the values of σ for Ti_2SC vary from about 0.2058 (consistent with the theoretical report 0.20,[26] 0.2035,[63] and 0.19,[28] as well as experimental measurement 0.16[28]) to 0.3325 in the pressure range of 0–200 GPa (see Fig. 7). It means that a higher ionic or weaker covalent contribution in intra-atomic bonding for Ti_2SC should be assumed.

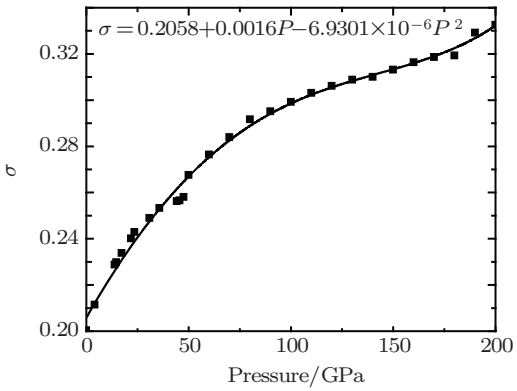


Fig. 7. Poisson's ratio of Ti_2SC as a function of pressure at 0 K.

Besides, for covalent and ionic materials, the typical relations between bulk and shear moduli are $G \approx 1.1B$ and $G \approx 0.6B$, respectively. For our case the calculated values of G/B are in the interval from 0.7489 at 0 GPa to 0.3771 at 200 GPa, which indicates that the ionic bonding is more suitable for Ti_2SC. On the other hand, to evaluate material ductility or brittleness, Pugh[64] introduced the B/G ratio: the material is brittle if the ratio is less than the critical value (1.75) or the material is ductile if the ratio G/B is below 0.57. In particular, it is evident that our Ti_2SC samples are brittle which is consistent with the available theoretical result[26] obtained from the ratio[24,65] of B/C_{44} with a value of 1.3353 under ambient conditions (see Fig. 8). Moreover, the current B/C_{44} is 1.17, below the typical members of M_2AX phases 1.2–1.7, also meaning that Ti_2SC samples may be more brittle under ambient conditions. However, the brittleness decreased with pressure, for instance, the B/G rises to 2.6519 at 200 GPa.

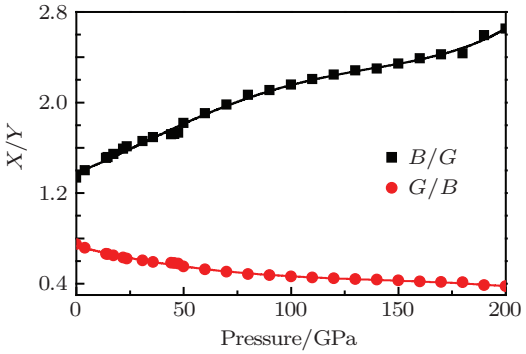


Fig. 8. (colour online) Brittleness and ductileness of Ti_2SC as a function of pressure at 0 K.

The thermodynamic properties of Ti_2SC are obtained by the quasi-harmonic Debye model, in which the phonon effects are considered, the calculated details can be seen elsewhere.[66] From which we have investigated many important thermodynamic properties. The Debye temperature is a fundamental parameter of a material, linked to many physical properties such as specific heat, elastic constants, and melting point. The Debye temperature at various temperatures and pressures is presented in Fig. 9. Our calculated Debye temperature at $T = 0$ K is 808.95 K, which is in agreement with the theoretical result 800 K[63] and slightly larger than the experimental measurement 631 K,[67] 765(15) K[28] and 745 K[28] as well as the DFT result 735 K.[28] From Fig. 9, we can obtain: (a) When the pressure remains constant (0, 60, 120, and 180 GPa), the Debye temperature almost linearly decreases with temperature. Moreover, the Debye temperature increases with the pressures and the increment decreased with the same pressure interval. Again, it is found that the Debye temperature decreased very slowly with temperatures under higher pressure. (b) When the temperature keeps constant (0, 600, and 1800 K), the Debye temperature almost linearly increases with applied pressures. Moreover, the Debye temperature at 1800 K is slightly lower than that at 0 K and the discrepancy seems to disappear under higher pressures. The current investigations demonstrated that the Debye temperature shows strong pressure and weak temperature dependences.

The Grüneisen parameter at various temperatures and pressures is presented in Fig. 10. From which we can obtain: (a) When the pressure keeps constant, the Grüneisen parameter almost linearly decreases with applied temperatures at 0 GPa, whereas the Grüneisen parameter behaves with a very slight increase at higher temperatures and the dependence decreased under higher pressures. (b) When the temperature keeps constant, the Grüneisen parameter almost linearly decreases with applied pressures only except an increase under pressure below 14 GPa. The discrepancy between different temperatures under the same pressure is very small, particularly under higher pressures, as is consistent with the case of the Debye temperature.

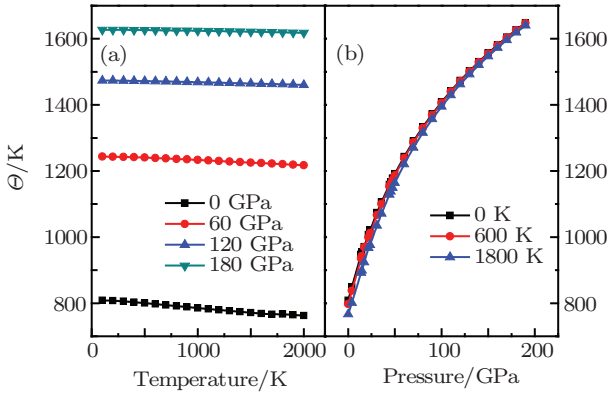


Fig. 9. (colour online) Debye temperature of Ti_2SC as a function of external conditions (P, T) under (a) different pressures and (b) different temperatures.

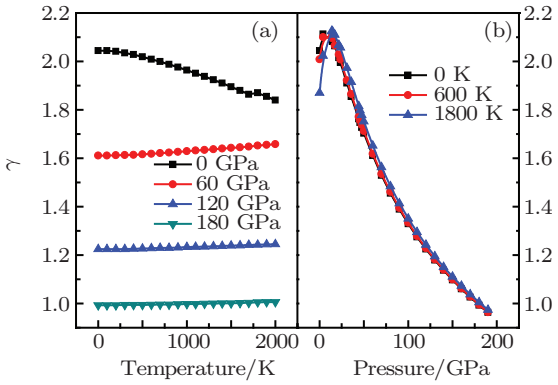


Fig. 10. (colour online) Grüneisen parameter of Ti_2SC as a function of external conditions (P, T) under (a) different pressures and (b) different temperatures.

The thermal expansion coefficient (α) variations with temperatures and pressures for Ti_2SC is presented in Fig. 11. From Fig. 11(a) it is clearly seen that α increases rapidly at low temperatures and the increasing trend becomes gentler. The effects of pressure on the thermal expansion coefficient are smaller at low temperatures than at high temperatures. In Fig. 11(b), as pressure increases, the thermal expansion coefficient decreases rapidly and the pressure dependence decreases. Moreover, the discrepancy at 1200 and 1800 K is small and the high temperature response is rapidly decreased. By further analysis of Figs. 11(a) and 11(b), we found that thermal expansion coefficient has experienced rapid changes at lower temperature (below 500 K) and pressure (below 50 GPa), and the lower the temperature/pressure is,

the faster the thermal expansion coefficient changes. It can be found that the thermal expansion coefficient converges to a constant value at high temperatures and high pressures. Figure 11 reveals the strong low temperature and pressure dependences of the thermal expansion coefficient.

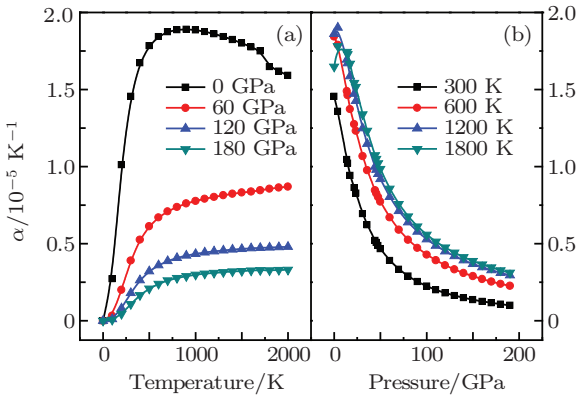


Fig. 11. (colour online) Thermal expansion coefficient of Ti_2SC as a function of external conditions (P, T) under (a) different pressures and (b) different temperatures.

According to the Debye temperature, we can calculate the lattice entropy (S) under different pressures and temperatures, as is shown in Fig. 12. From which we can see that: (a) When the pressure keeps constant, the lattice entropy increases monotonously with temperature. (b) When the temperature keeps constant, the lattice entropy decreases monotonously with pressure. The current investigations demonstrated that the lattice entropy behaves with strong pressure and temperature dependence.

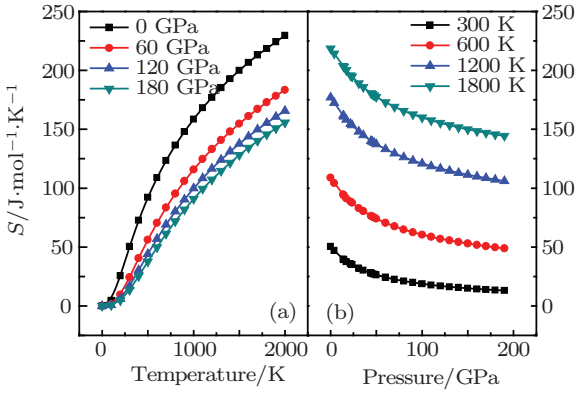


Fig. 12. (colour online) Lattice entropy of Ti_2SC as a function of external conditions (P, T) under (a) different pressures and (b) different temperatures.

The heat capacity at constant pressure C_P and heat capacity at constant volume C_V with temperature T and pressure P are systematically investigated to clarify their subtle discrepancy in a solid substance as the present Ti_2SC has behaved with weak higher temperature responses, as is shown in Fig. 13. As we all know, the difference between C_P and C_V is very small under low temperatures. However, under high temperatures, the C_V approaches a constant value, C_P increases monotonously with temperature. The values follow the Debye model under low temperature ($C_V(T)$–T^3) and the classical behavior ($C_V(T)$–$3R$ for mono-atomic solids) is found under high enough temperatures, obeying the Dulong–Petit's limit rule. From Fig. 13 one could see that the discrepancy between the C_P and C_V is negligible until up to 200 GPa under lower temperatures (such as below 300 K), whereas the discrepancy increases with temperatures (as the plot at 600, 1200, and 1800 K). Moreover, the temperature induced discrepancy decreases with pressure, and the larger discrepancy can only be found above 1200 K.

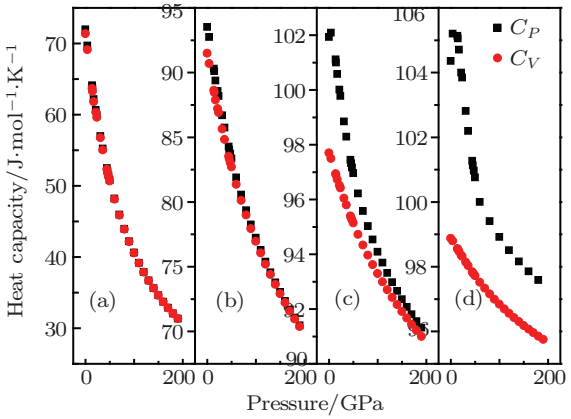


Fig. 13. (colour online) Heat capacity of Ti_2SC varies with pressure under different temperatures: (a) 300 K, (b) 600 K, (c) 1200 K, (d) 1800 K.

From Fig. 14 we see that both the C_V and C_P increase with temperature at 0 GPa. Meanwhile, the temperature dependence of the C_V and C_P are calculated and show reasonable agreement with experimental measurement[67] (only except the evident discrepancy with the experiment for C_P under higher temperatures, including the present calculated results and other available theoretical results.[67]) From the current investigations we found that the discrepancy between C_V and C_P is small under lower temperatures and increases with temperature. On the other hand, the discrepancy decreases with pressure, such that the discrepancy could be reasonably neglected at 180 GPa under the whole temperature range of 0–2000 K. By comparing C_V and C_P, we found that C_P has experienced stronger pressure dependences particularly at higher temperatures.

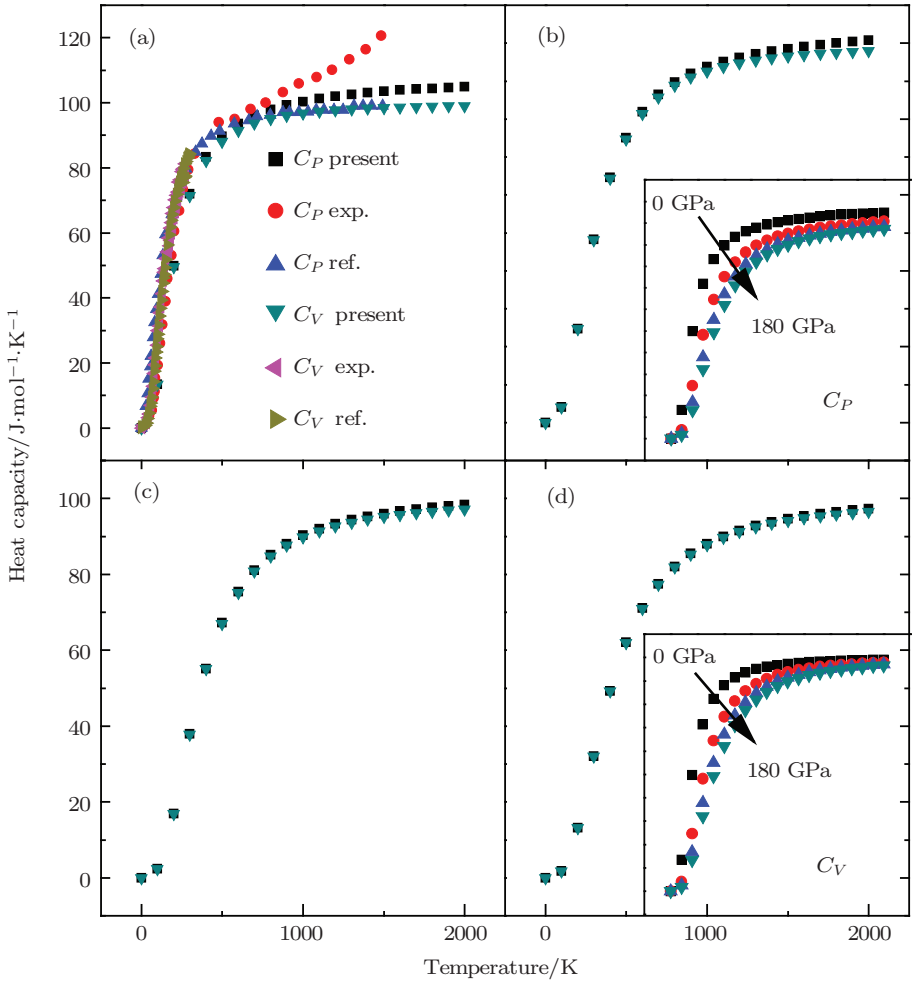


Fig. 14. (colour online) Heat capacity of Ti_2SC varies with temperature under different pressures, the experimental and theoretical data are taken from Ref. [69] (a) 0 GPa, (b) 60 GPa, (c) 120 GPa, (d) 180 GPa.

4. Conclusions

We have performed comprehensive elastic and thermodynamic property investigations for Ti_2SC for the first time. Our calculations on elastic constants demonstrated that Ti_2SC is stable up to 200 GPa and no phase transition has been detected. The structural coordinate parameter investigations of the Ti atom confirmed its pressure dependence. The Poisson's ratio calculations demonstrated that a higher ionic or weaker covalent contribution in intra-atomic bonding for Ti_2SC should be assumed and the nature of ionic increases with pressure. Moreover, the G/B and B/C_{44} also revealed that Ti_2SC is brittle and the brittleness decreases with pressure. The heat capacities C_V and C_P investigations show that the discrepancy between them is very small under lower temperatures (below 300 K), whereas the discrepancy increased with temperature under low pressure and decreased under high pressure. Our calculations further exhibit that the adiabatic bulk moduli B_S increases with temperature at 0 GPa and then decreases under higher pressures. In contrast with B_S, the isothermal bulk modulus B_T displayed similar variation tendencies with the only exception of a minimum value at zero pressure. The current investigations confirmed that B_S is always larger than B_T over wide pressure/temperature ranges and both of them increase with temperature at 0 GPa. Moreover, we have extensively studied Debye temperature, Grüneisen parameter, thermal expansion coefficient and entropy. Analysis of the above four quantities suggests that they have displayed strong pressure and certain temperature dependences with the only exceptions of Debye temperature and Grüneisen parameter as both of them have experienced very weak temperature responses.

References

[1] Barsoum M W 2000 *Prog. Solid State Chem.* **28** 201

[2] Yoo H, Barsoum M W and Ei-Raghy T 2000 *Nature* **407** 581

[3] Finkel P, Hettinger J D, Lofland S E, Barsoum M W and Ei-Raghy T 2001 *Phys. Rev.* B **65** 035113

[4] Lofland S E, Hettinger J D, Meehan T, Bryan A, Finkel P, Gupta S, Barsoum M W and Hug G 2006 *Phys. Rev.* B **74** 174501

[5] Barsoum M W, Radovic M, Zhen T, Finkel P and Kalidindi S R 2005 *Phys. Rev. Lett.* **94** 085501

[6] Barsoum M W, Murugaiah A, Kalidindi S R and Zhen T 2004 *Phys. Rev. Lett.* **92** 255508

[7] Ivanovskii A L 1996 *Uspekhi Khimii* **65** 499

[8] Sun Z M, Ahuja R and Schneider J M 2003 *Phys. Rev.* B **68** 224112

[9] Barsoum M W and Ei-Raghy T 1996 *J. Am. Ceram. Soc.* **79** 1953

[10] Barsoum M W, Brodkin D and Ei-Raghy T 1997 *Scr. Metall. Mater.* **36** 535

[11] Li J F, Pan W, Sato F and Watanabe R 2001 *Acta Mater.* **49** 937

[12] Amini S, Barsoum M W and Ei-Raghy T 2007 *J. Am. Ceram. Soc.* **90** 3953

[13] Medvedeva N I and Freeman A J 2008 *Scripta Mater.* **58** 671

[14] Toth L E, Jeitschko W and Yen M 1967 *J. Less Common Met.* **10** 129

[15] Sakamaki K, Wada H, Nozaki H Y, Onuki Y and Kawai M 1999 *Solid State Commun.* **112** 323

[16] Bortolozo A D, Sant'anna O H, Luz M S D, Santos C A M D, Pereira A S, Trentin K S and Machado A J S 2006 *Solid State Commun.* **139** 57

[17] Bortolozo A D, Sant'anna O H, Santos C A M D and Machado A J S 2007 *Solid State Commun.* **144** 419

[18] Gao G Y, Oganov A R, Li P F, Li Z W, Wang H, Cui T, Ma Y M, Bergara A, Lyakhov A O, Litaka T and Zou G T 2010 *Proc. Natl. Acad. Sci. USA* **107** 1317

[19] Lv J, Wang Y C, Zhu L and Ma Y M 2011 *Phys. Rev. Lett.* **106** 015503

[20] Ma Y M, Eremets M, Oganov A R, Xie Y, Trojan I, Medvedev S, Lyakhov A O, Valle M and Prakapenka V 2009 *Nature* **458** 182

[21] Li Q, Ma Y M, Oganov A R, Wang H B, Wang H, Xu Y, Cui T, Mao H K and Zou G T 2009 *Phys. Rev. Lett.* **102** 175506

[22] Gupta S, Amini S, Filimonov D, Palanisamy T, Ei-Raghy T and Barsoum M W 2007 *J. Am. Ceram. Soc.* **90** 3566

[23] Du Y L, Sun Z M, Hashimoto H and Tian W B 2008 *Solid State Commun.* **145** 461

[24] Sun Z M, Li S, Ahuja R and Schneider J M 2004 *Solid State Commun.* **129** 589

[25] Hug G 2006 *Phys. Rev.* B **74** 184113

[26] Du Y L, Sun Z M, Hashimoto H and Tian W B 2008 *Phys. Lett.* A **372** 5220

[27] Cui S X, Feng W X, Hu H Q, Feng Z B and Liu H 2009 *Scripta Mater.* **61** 576

[28] Scabarozi T H, Amini S, Finkel P, Leaffer O D, Spanier J E, Barsoum M W, Drulis M, Drulis H, Tambussi W M, Hettinger J D and Lofland S E 2008 *J. Appl. Phys.* **104** 033502

[29] Kulkarni S R, Vennila R S, Phatak N A, Saxena S K, Zhab C S, El-Raghy T, Barsoumd M W, Luoe W and Ahuja R 2008 *J. Alloys Comp.* **448** L1

[30] Chen Y H, Du R, Zhang Z L, Wang W C, Zhang C R, Kang L and Luo Y C 2011 *Acta Phys. Sin.* **60** 086801 (in Chinese)

[31] Cheng Z M, Wang X Q, Wang F, Lu L Y, Liu G B, Duan Z F and Nie Z X 2011 *Acta Phys. Sin.* **60** 096301 (in Chinese)

[32] Fan K M, Yang L, Peng S M, Long X G, Wu Z C and Zu X T 2011 *Acta Phys. Sin.* **60** 076201 (in Chinese)

[33] Hu Y P, Ping K B, Yan Z J, Yang W and Gong C W 2011 *Acta Phys. Sin.* **60** 107504 (in Chinese)

[34] Liu C H, Ouyang C Y and Ji Y H 2011 *Acta Phys. Sin.* **60** 077103 (in Chinese)

[35] Liu F L, Jiang G, Bai L N and Kong F J 2011 *Acta Phys. Sin.* **60** 567 (in Chinese)

[36] Liu J J 2011 *Acta Phys. Sin.* **60** 555 (in Chinese)

[37] Ru Q, Hu S J and Zhao L Z 2011 *Acta Phys. Sin.* **60** 448 (in Chinese)

[38] Wang F, Wang X Q, Nie Z X, Cheng Z M and Liu G B 2011 *Acta Phys. Sin.* **60** 480 (in Chinese)

[39] Wang X Z, Lin L B, He J and Chen J 2011 *Acta Phys. Sin.* **60** 077104 (in Chinese)

[40] Wen L W, Wang Y M, Pei H X and Jun D 2011 *Acta Phys. Sin.* **60** 599 (in Chinese)

[41] Yuan D, Luo H F, Huang D H and Wang F H 2011 *Acta Phys. Sin.* **60** 077101 (in Chinese)

[42] Zhang H, Zhang G Y, Xiao M Z, Lu G X, Zhu S L and Zhang K 2011 *Acta Phys. Sin.* **60** 593 (in Chinese)

[43] Zhang Y J, Yan J L, Zhao G and Xie W F 2011 *Acta Phys. Sin.* **60** 560 (in Chinese)

[44] Li Y W and Ma Y M 2010 *SCIENTIA SINICA Phys, Mech & Astron* **40** 146 (in Chinese)

[45] Li Q and Ma Y M 2011 *Prog. Chem.* **23** 829

[46] Hao A M, Zhou T J, Zhu Y, Zhang X Y and Liu R P 2011 *Chin. Phys.* B **20** 047103

[47] Li X F, Zhai H C, Fu H Z, Liu Z L and Ji G F 2011 *Chin. Phys.* B **20** 093101

[48] Liu C M, Ge N N, Fu Z J, Cheng Y and Zhu J 2011 *Chin. Phys.* B **20** 045101

[49] Xu Y J Z, Shang J X and H.Wang F 2011 *Chin. Phys.* B **20** 037101

[50] Zhang L, Ji G F, Zhao F and Gong Z Z 2011 *Chin. Phys.* B **20** 047102

[51] Vanderbilt D 1990 *Phys. Rev.* B **41** 7892

[52] Perdew J P, Burke K and Ernzerhof M 1996 *Phys. Rev. Lett.* **77** 3865

[53] Hammer B, Hansen L B and Norskov J K 1999 *Phys. Rev.* B **59** 7413

[54] Payne M C, Teter M P, Allen D C, Arias T A and Joannopoulos J D 1992 *Rev. Mod. Phys.* **64** 1045

[55] Milman V, Winkler B, White A, Packard C J, Payne M C, Akhmatskaya E V and Nobes R H 2000 *Int. J. Quantum. Chem.* **77** 895

[56] Bouhemadou A 2009 *Appl. Phys.* A **96** 959

[57] Monkhorst H J and Pack J D 1976 *Phys. Rev.* B **13** 5188

[58] Born M 1940 *Proc. Cambridge Philos. Soc.* **36** 160

[59] Islam A K M A, Sikder A S and Islam F N 2006 *Phys. Lett.* A **350** 288

[60] Auld M A 1973 *Acoustic Fields and Waves in Solids* (New York: Wiley)

[61] Neumann G S, Stixtude L and Cohen R E 1999 *Phys. Rev.* B **60** 791

[62] Haines J, Leger J M and Bocquillon G 2001 *Annu. Rev. Mater. Res.* **31** 1

[63] Bouhemadou A and Khenata R 2008 *Phys. Lett.* A **372** 6448

[64] Pugh S F 1954 *Philos. Mag.* **45** 833

[65] Holm B, Ahuja R and Johannson B 2001 *Appl. Phys. Lett.* **79** 1450
[66] Blanco M A, Francisco E and Luana V 2004 *Comp. Phys. Comm.* **158** 57
[67] Drulis M K, Drulis H, Hackemer A E, Leaffer O, Spanier J, Amini S, Barsoum M W, Guilbert T and Raghy T E 2008 *J. Appl. Phys.* **104** 023526
[68] Barsoum M W, *Physical Properties of the MAX Phases, Encyclopedia of Materials: Science and Technology* (Elsevier, Amsterdam, 2006).
[69] Scabarozi T H, Amini S, Leaffer O, Ganguly A, Gupta S, Tambussi W, Clipper S, Spanier J E, Barsoum M W, Hettinger J D and Lofland S E 2009 *J. Appl. Phys.* **105** 013543
[70] Holm B, Ahuja R, Li S and Johansson B 2002 *J. Appl. Phys.* **91** 9874
[71] Du Y L, Sun Z M and Hashimoto H 2010 *Physica* B **405** 720
[72] Cover M F, Warschkow O, Bilek M M M and Mckenzie D R 2009 *J. Phys.: Condens. Matter* **21** 305403